

# Report: Synchronisation in Chaotic Systems

Sahaana Vijay

(Dated: July 26, 2024)

In this report, various coupled chaotic systems, such as the coupled logistic and tent map systems, have been studied in the context of weak (WS) and strong synchronisation (SS). Using the ideas from the paper ‘*Weak and Strong Synchronization of Chaos*’ by K. Pyragas [1], the dynamics of the systems, the variation of Lyapunov exponents with the coupling parameter  $k$  and finite-time Lyapunov exponents were explored. The plots in the paper were reproduced and analysed in connection to other coupled systems of 1D maps. This report compiles the observations and results found while studying these coupled systems.

## I. THE COUPLED LOGISTIC SYSTEM

### A. Coupled Systems and Synchronisation

In the conventional synchronisation of a chaotic system, we notice that the variables match each other as they evolve in the phase space. In contrast, in generalised synchronisation, the system states are related by a function or a map. Here, we will be considering a unidirectional master-slave system (coupled 1D maps  $x_{n+1}, y_{n+1}$ ) with an auxiliary response map ( $y'_{n+1}$ ) defined as

$$\begin{aligned}x_{n+1} &= f(x_n) \\y_{n+1} &= f(y_n) + kf(x_n) - f(y_n) \\y'_{n+1} &= f(y_n) + kf(x_n) - f(y'_n)\end{aligned}\tag{1}$$

with  $k$  being the coupling parameter.

In these coupled systems, the transition of the maps from being unsmooth to smooth is related to the synchronisation in the system. An unsmooth map indicates weak synchronisation (WS) and a smooth map indicates (SS). As the system evolves with  $k$ , we first notice WS between  $y$  and  $y'$  and later, we notice SS between  $x$  and  $y$  (essentially conventional synchronisation where both  $x$  and  $y$  collapse to an identity map). The threshold  $k$  values at which WS and SS are observed are characterised by the corresponding **conditional**  $\lambda_R$  and **transverse**  $\lambda_0$  Lyapunov exponents, defined by

$$\lambda_R = \ln(1-k) + \lim_{n \rightarrow \infty} \frac{1}{n} \sum_{i=1}^n \ln |f'(y_i)|\tag{2}$$

$$\lambda_0 = \ln(1 - k) + \lim_{n \rightarrow \infty} \frac{1}{n} \sum_{i=1}^n \ln |f'(x_i)|. \quad (3)$$

The conditional Lyapunov exponents for each of the  $k$  values determine the stability of the  $y-y'$  synchronisation, and the transverse Lyapunov exponents for each of the  $k$  values determine the stability of the  $x-y$  synchronisation. We get the threshold  $k$  values when  $\lambda_R$  and  $\lambda_0 \rightarrow 0$ . In the second term of the equations for conditional and transverse Lyapunov exponents,  $f'(x_i)$  or  $f'(y_i)$  can be found by orthogonalising the two vectors for every point on the trajectory using the Gram-Schmidt process and finding the norm of both the vectors. One can understand how chaotic a system is by looking at how wide apart these vectors get over time.

### B. Dynamics of a Coupled Logistic System

We defined the coupled logistic system, where  $f(x_n) = 4ax(1-x)$ , as

$$\begin{aligned} x_{n+1} &= 4ax(1-x) \\ y_{n+1} &= 4ay(1-y)(1-k) + 4akx(1-x) \\ y'_{n+1} &= 4ay'(1-y')(1-k) + 4akx(1-x) \end{aligned} \quad (4)$$

using equations (2) and (3). Considering  $a = 1$ , 1000 iterations and 500 transients, we can find the dynamics of the system at  $k = 0.1$  (unsynchronised case),  $k = 0.4$  (WS) and  $k = 0.6$  (SS) through phase plots for  $y-y'$  and  $x-y$  as shown in Figures. 1, 2, 3.

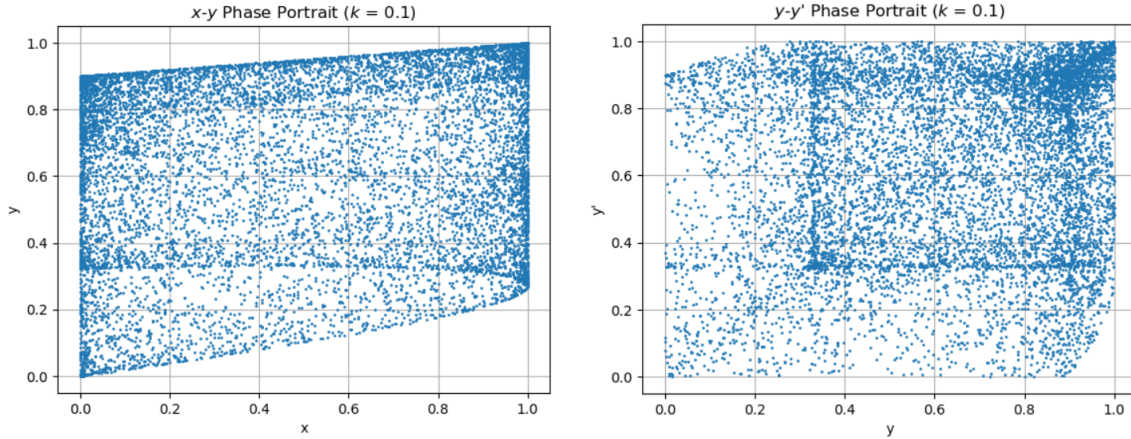


FIG. 1. Visualising the dynamics of a coupled logistic system through phase portraits: The above plots showcase the  $x-y$  and  $y-y'$  dynamics when the system is unsynchronised by taking  $k = 0.1$  and  $a = 1$ .

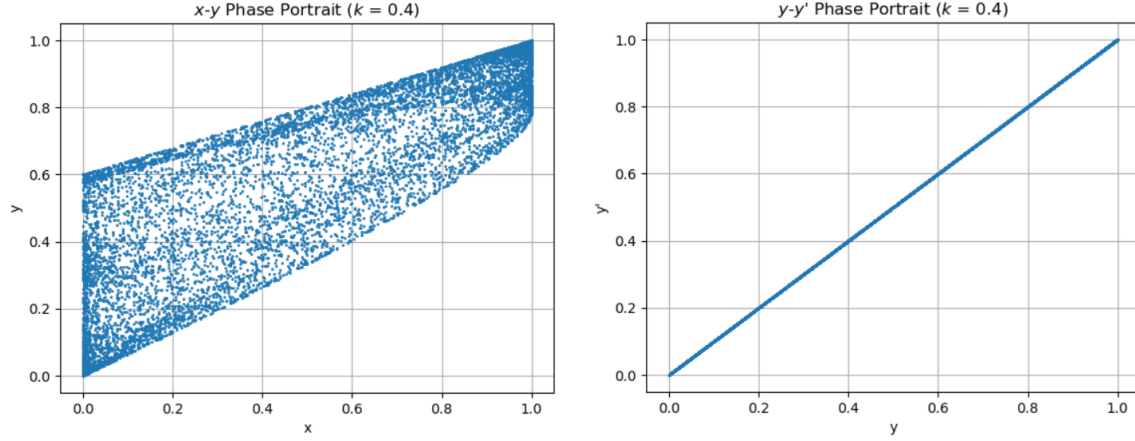


FIG. 2. Visualising the dynamics of a coupled logistic system through phase portraits: The above plots showcase the  $x$ - $y$  and  $y$ - $y'$  dynamics when the system is weakly synchronised at  $k = 0.4$  and  $a = 1$ . Here, we notice that when the system is weakly synchronised, the values of  $y$  and  $y'$  collapse to an identity map (as mentioned earlier) and match each other. In practical situations, one can observe noise in the synchronisation of  $y$  and  $y'$ .

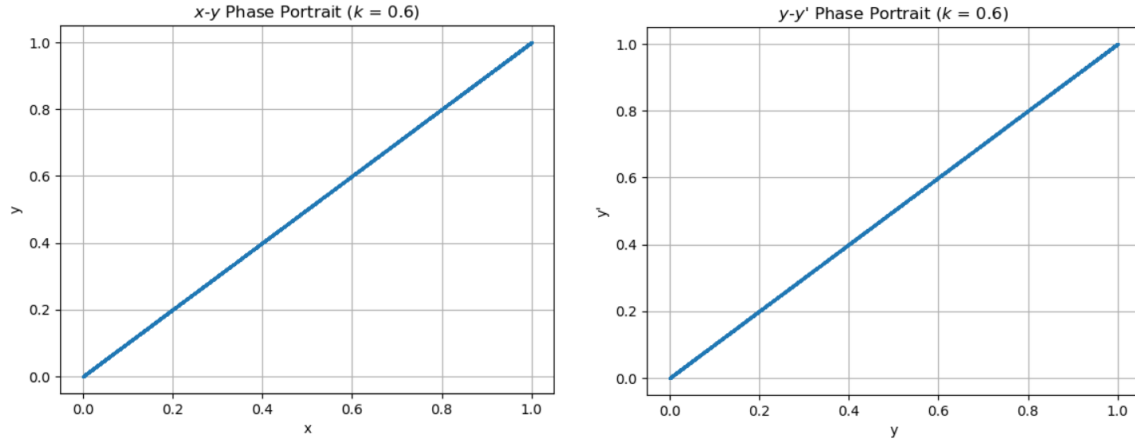


FIG. 3. Visualising the dynamics of a coupled logistic system through phase plots: The above plots showcase the  $x$ - $y$  and  $y$ - $y'$  dynamics when the system is strongly synchronised at  $k = 0.6$  and  $a = 1$ . In these plots, we can see that when the system is strongly synchronised, the values of  $x$  and  $y$  also match.

### C. Lyapunov Analysis

The algorithm to evaluate the Lyapunov exponents first involves obtaining the vectors for every point on the trajectory by multiplying the Jacobian matrix of the system with the original basis vectors and then using the Gram-Schmidt process to orthogonalise them. We do this because even though the original basis vectors  $\hat{i}$  and  $\hat{j}$  are orthogonal, the vectors at each point on the trajectory

may not be. After this, we can find the norm of the vectors, and these are our values for  $f'(x_i)$  or  $f'(y_i)$ . Finally, we apply equations (2) and (3) to find the exponents for each of the  $k$  values. By taking a set of 1000  $k$  values ranging from 0.0 to 1.0, iterating the system 10000 times (500 transient iterations) for each of the  $k$  values, and applying the algorithm, the conditional and transverse Lyapunov exponents were computed for the coupled logistic map system (Figure. 4).

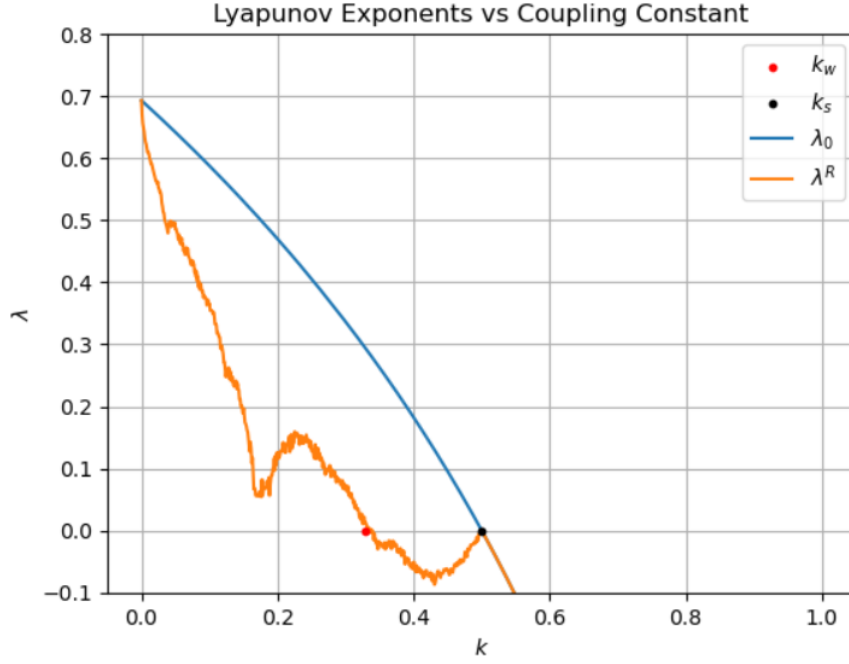


FIG. 4. Plotting the conditional (orange-coded) and transverse (blue-coded) Lyapunov exponents against each of the 1000  $k$  values considered with randomised initial conditions for the system. The points at which the curves cross the  $x$ -axis give us the thresholds for WS and SS, i.e.,  $k_w$  and  $k_s$ . Here, the thresholds for the system are estimated to be  $k_w = \mathbf{0.328}$  and  $k_s = \mathbf{0.500}$  as they were found by eyeballing.

To further investigate how the Lyapunov exponents vary with the coupling parameter  $k$ , the entire process was repeated for the same number of iterations and  $k$  values 30 times, and the Lyapunov exponents data obtained after every iteration of the entire process were stored in `.csv` files. Using this data, the average of each of the Lyapunov exponents and the  $k$  values were calculated, following which the derivative of each of the Lyapunov exponents was computed with respect to the  $k$  values. Then, the derivatives were plotted against the  $k$  as shown in Figure. 5. An interesting observation is that the derivative of the Lyapunov exponent exhibits considerable variability until  $k = k_w = 0.328$ . Beyond this threshold, the variability decreases, indicating WS in the system. Subsequently, after reaching the threshold  $k = k_s = 0.500$ , the transition becomes more abrupt. Comparing this behaviour to Figure 4, we can say that as  $k_s$  marks a critical point for SS in the

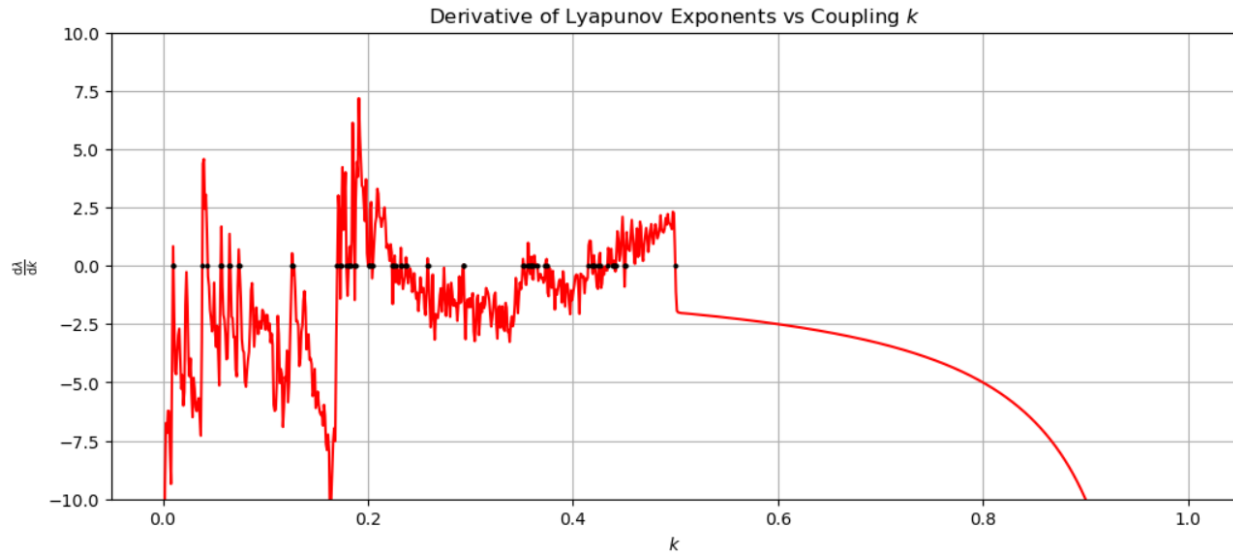


FIG. 5. Plotting the derivative of the Lyapunov exponents against the coupling parameter  $k$ . The points marked in black indicate  $\frac{d\lambda}{dk} = 0$

system, characterised by an abrupt change followed by a reduction in chaotic behaviour, we see a similar pattern in the derivatives as well. Another interesting thing to note is that in Figure. 4, after  $k_w$ , the Lyapunov exponent becomes negative (stable) and rises until it reaches  $k_s$ .

There are three segments of Figure. 5 that one can study here – the segments between  $k = 0.0$  and  $0.2$ ,  $0.2$  and  $0.4$ , and between  $0.4$  and  $0.6$ . We can study these segments through the lens of *finite-time Lyapunov exponents* (FTLE). To find the FTLE for the system, we can first generate a set of data points for  $x$ ,  $y$ , and  $y'$ , and divide them into various chunks. Then, the conditional Lyapunov exponents for each chunk at a given  $k$  value can be found and visualised through a histogram. The average of the values gives us the Lyapunov exponent at that  $k$  value for the system. In our case, 50000 data points were generated and were divided into 500 chunks of 100 data points. The Lyapunov exponents for the chunks were calculated for  $k = 0.024$  (the second prominent maximum in the first segment),  $k = 0.182$  (the global maximum; note that these are approximate  $k$  values), and the two thresholds.

The variance in the Lyapunov exponents for each of the  $k$  values can be plotted against the  $k$  values. In Figure. 8, one can see that the variance practically becomes zero and continues to remain that way without many perturbations due to strong synchronisation. Additionally, the peak in the graph corresponds to the peak in the derivative in Figure. 5 at around the same value, i.e., just before  $k = 0.2$ .

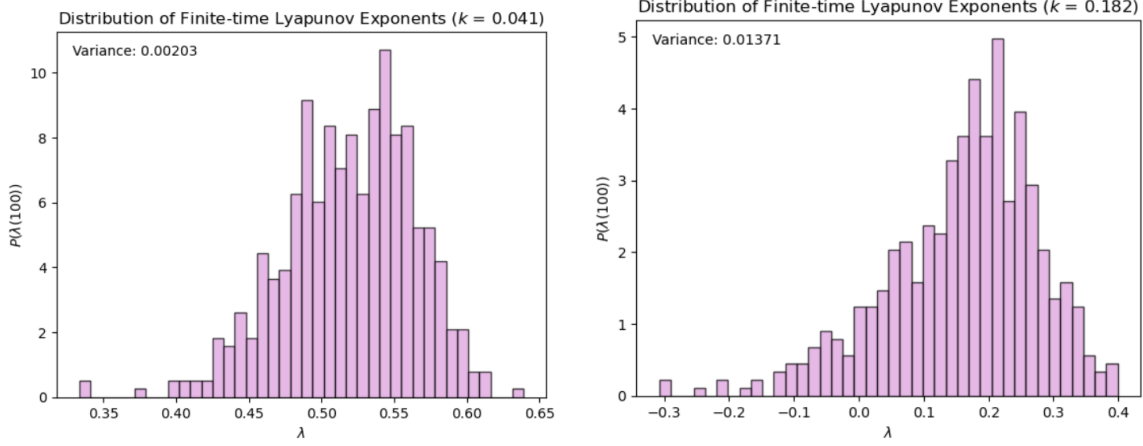


FIG. 6. Histogram of finite-time Lyapunov exponents for  $k = 0.041$  and  $k = 0.182$

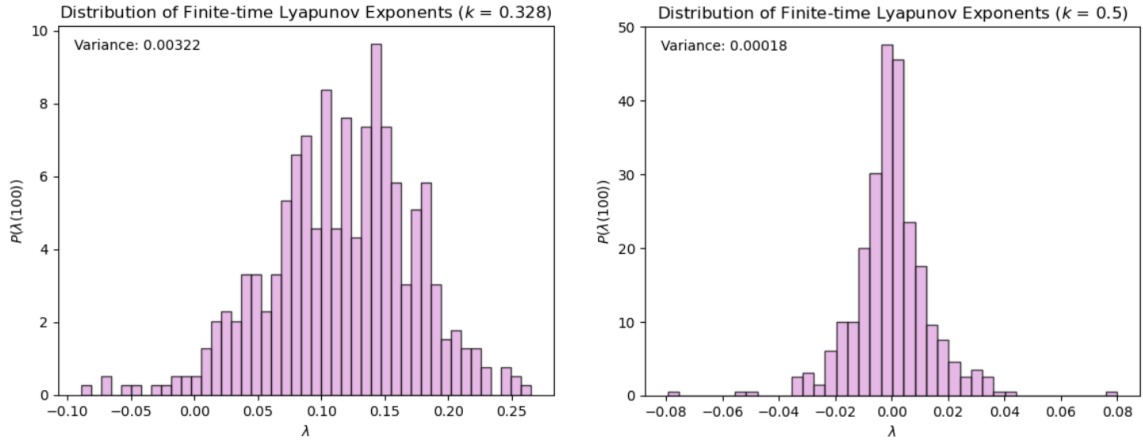


FIG. 7. Histogram of finite-time Lyapunov exponents for  $k = 0.328$  and  $k = 0.500$

#### D. Miscellaneous Properties of the System

At the threshold  $k_w$ , we have  $y = f(x)$  that is not smooth and has a complex fractal structure. So, we can find the correlation dimension  $d_c$  and plot it against  $k$  to understand the complexity of the attractor in the  $x$ - $y$  plane. To do this, the Grassberger-Procaccia algorithm [2] was used by first writing a function to calculate the *correlation sum*  $C(\epsilon)$ , which is the average number of pairs of points within a distance  $\epsilon$  (nearest neighbours found using cKDTree) in a phase space. Then,  $d_c$  was calculated by finding the slope of the log-log plot of the correlation sum  $C(\epsilon)$  versus  $\epsilon$ . The correlation dimension was calculated for 50000 data points (the same as the number of data points in Pyragas' paper).

The mean local *thickness*  $\sigma$  of the map was also evaluated and plotted against  $k$  to check

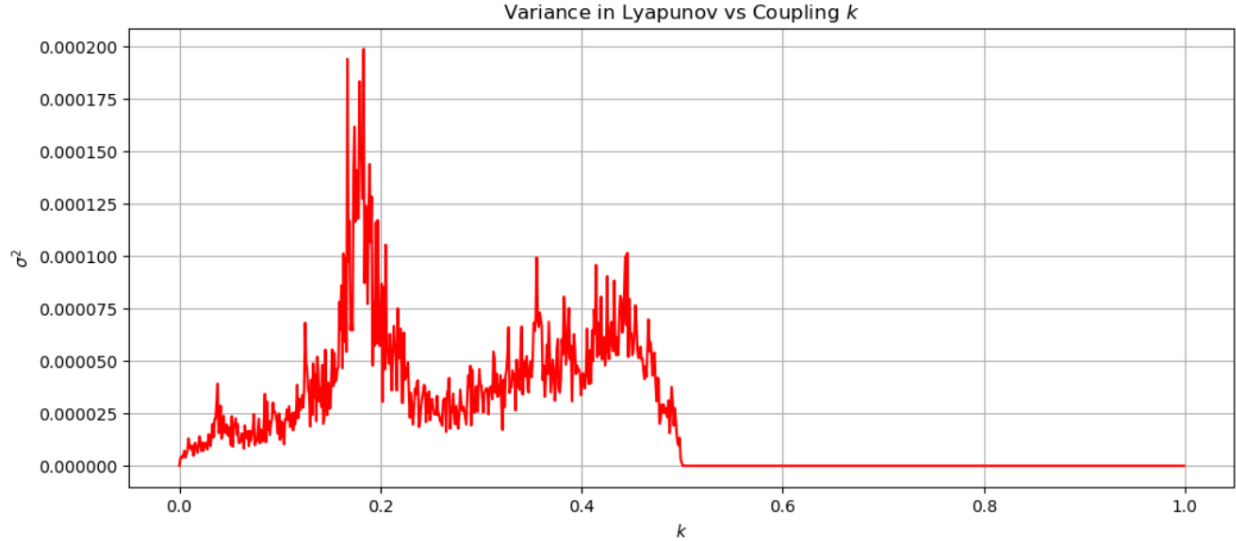


FIG. 8. Plotting the variance in the Lyapunov exponents against the corresponding  $k$  values. This was done for 30 datasets, and the average was plotted against  $k$ .

the smoothness of the map, as  $\sigma$  measures how much the points deviate from the local linear interpolation. The thickness vs.  $k$  was replicated using the same parameters in Pyragas' paper. Within a small neighbourhood  $\epsilon = 0.001$  around a given point  $x = x_i$ , a local linear interpolation was applied to the map  $y = f(x)$  using the least squares fit. The local mean square deviations were averaged over  $N = 5000$  randomly chosen points on the attractor, and the square root of this average value gave us the thickness  $\sigma$ . The total number of data points is  $N = 50000$ . The cross-correlator  $K_{xy}$  was plotted on the graph against the coupling strength  $k$  (see Figure. 9).

## II. COMPARISON WITH OTHER COUPLED SYSTEMS OF 1D MAPS

### A. Coupled Tent Map

The tent map is defined as

$$f(x, \mu) = \begin{cases} \mu x & \text{if } x < 0.5 \\ \mu(1 - x) & \text{if } x \geq 0.5 \end{cases} \quad (5)$$

and in our case,  $\mu$  was taken as 1.99. First, the conditional and transverse Lyapunov exponents were calculated for the coupled system created by incorporating equation (5) into (1) and the exponents were again plotted against  $k$  like how it was done for the coupled logistic map.

Looking at the 10, the thresholds for WS and SS were almost equal, so the dynamics/phase

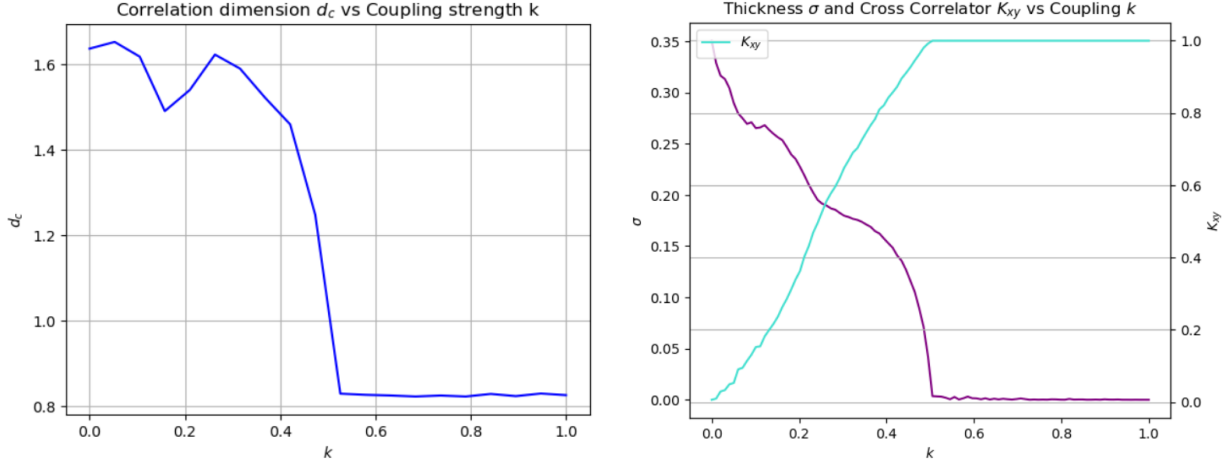


FIG. 9. (Left) Plotting the correlation dimension against  $d_c$  against coupling  $k$ . Here, one can observe that when we reach the threshold  $k_w$ , there is no noticeable change in  $d_c$ . The dimension decreases sharply only at  $k_s$  where the relation  $f$  becomes an identity function. (Right) Plotting the thickness  $\sigma$  and cross-correlator  $K_{xy}$  against  $k$ . In this plot, we can see there are no significant changes at  $k_w$ , however, the curve decreases sharply at  $k_s$  as it becomes smoother.

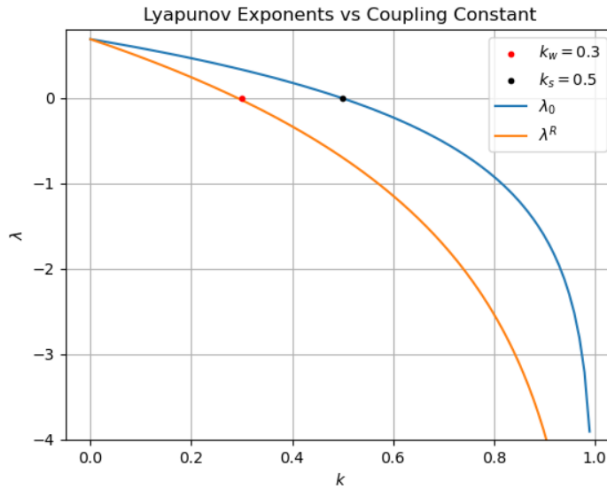


FIG. 10. Plotting the conditional and transverse Lyapunov exponents against the coupling strength  $k$  for the coupled tent map. Interestingly, from the graph, we can see that the thresholds for  $k_w$  and  $k_s$  are very close to the values of the thresholds for the coupled logistic map.

portraits for the neighbourhood ( $k - \epsilon$  and  $k + \epsilon$ ) were plotted by varying  $\epsilon$  from  $10^{-5}$  to 0.01 in powers of 10 in Figures. 11, 12, 13, to explore this coincidence in detail. In the phase portraits, one can note that the dynamics at these points seem very similar to the dynamics of the coupled logistic map, and so, we went on to plot the dynamics at these thresholds over the dynamics of the

coupled logistic system (Figure 14). When comparing the  $x$ - $y$  dynamics of both coupled tent and logistic maps, it is observed that the data points follow each other closely, which is why they have similar thresholds for WS and SS.

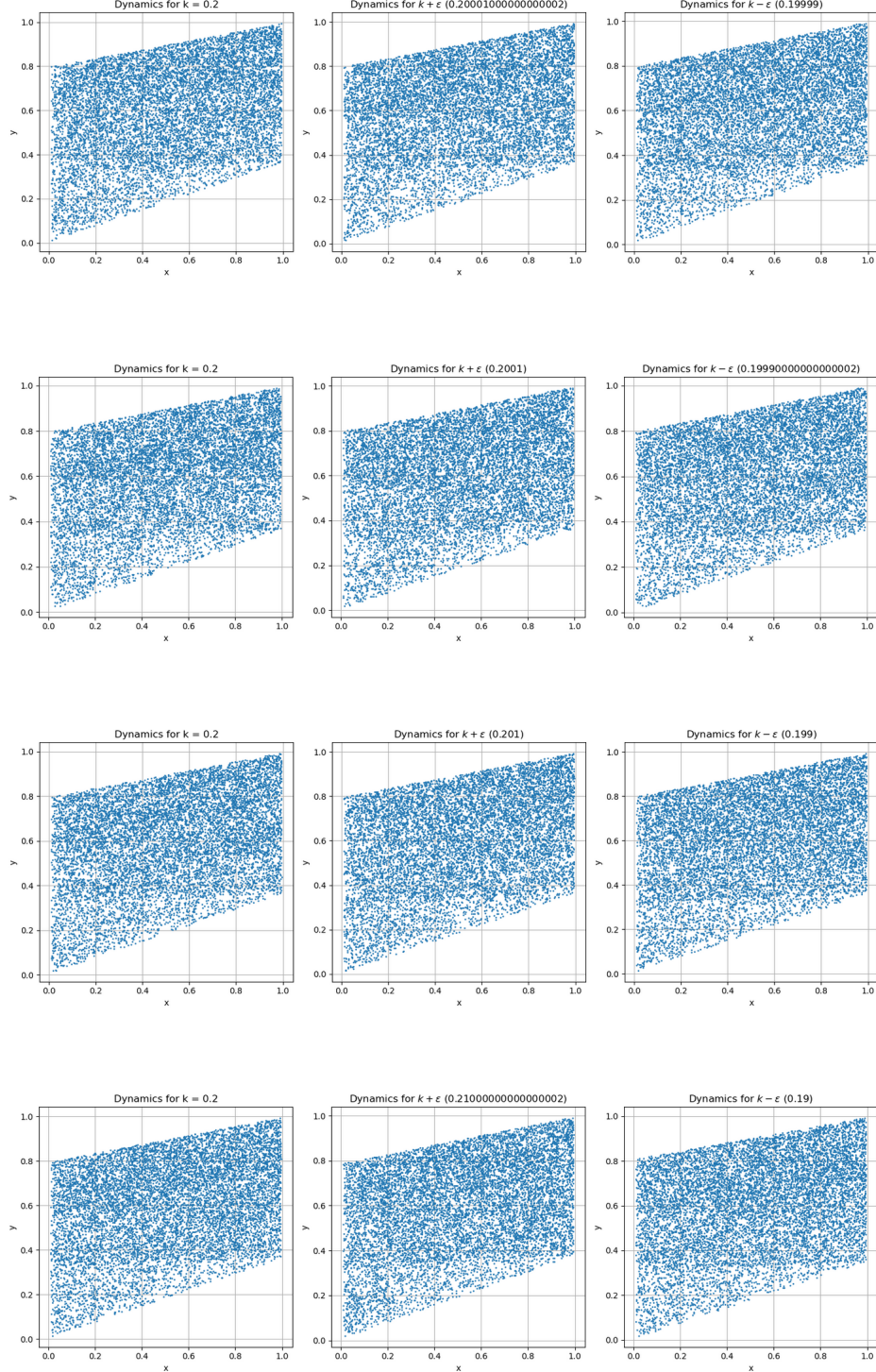


FIG. 11. The  $x$ - $y$  dynamics of the coupled tent map system at  $k = 0.2$ , i.e., when the system is unsynchronised.

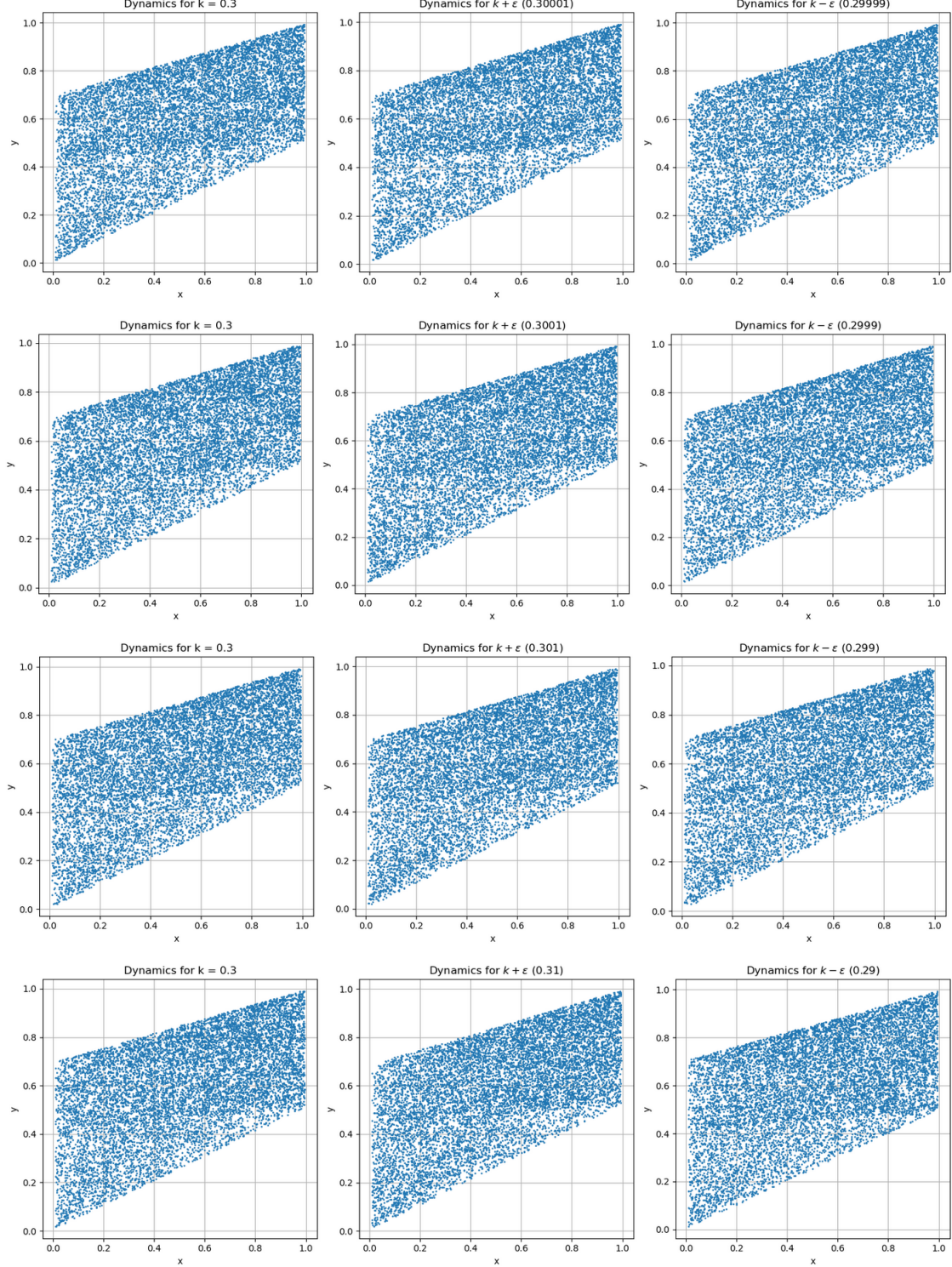


FIG. 12. The  $x$ - $y$  dynamics of the coupled tent map system at  $k = 0.3$ , i.e., when the system is weakly synchronised.

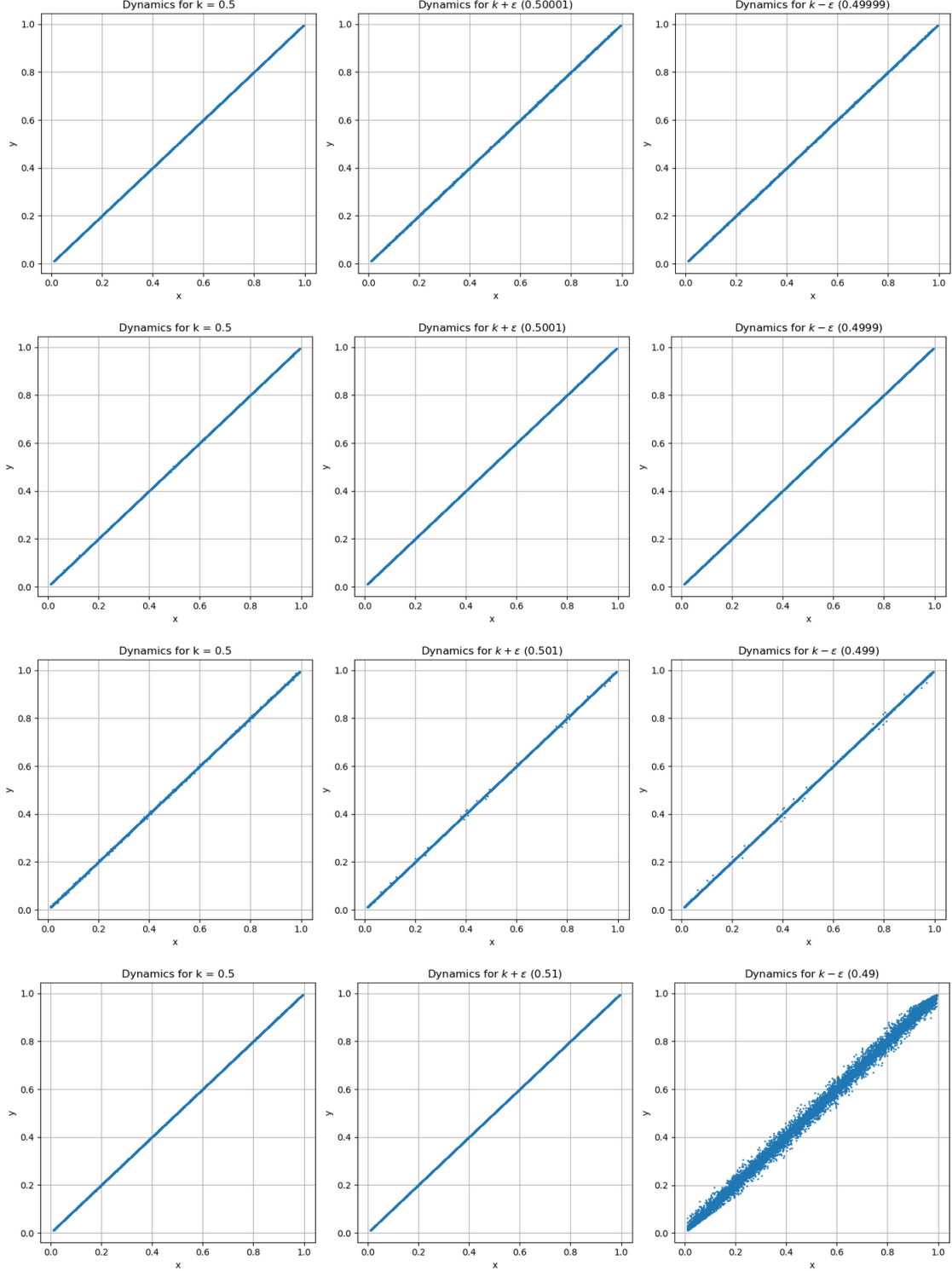


FIG. 13. The  $x$ - $y$  dynamics of the coupled tent map system at  $k = 0.5$ , i.e., when the system is strongly synchronised.

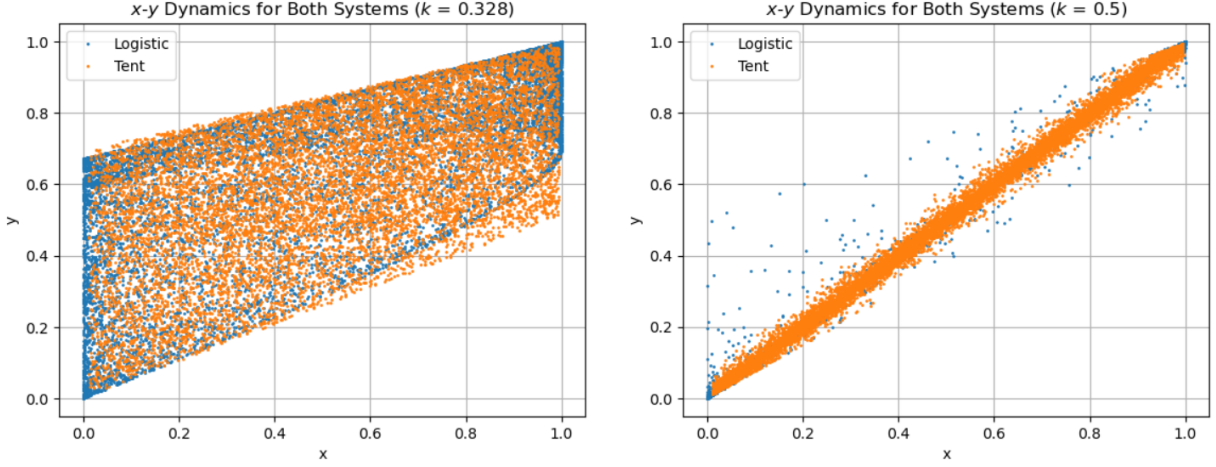


FIG. 14. (Left) Overlapping the  $x$ - $y$  phase portraits for the coupled logistic and tent maps at  $k_w = 0.3$  to see the similarity in dynamics. (Right) Overlapping the  $x$ - $y$  phase portraits for the coupled logistic and tent maps at  $k_s = 0.5$ . In both plots, we can see that the dynamics are almost the same for both systems at these points.

### B. Coupled Sine Map

The sine map is given by  $f(x_n) = x_{n+1} = r \sin(\pi x_n)$  where we will consider  $r = 0.9$  as we can observe chaotic behaviour at that value. Plugging this into equation (1), we obtain the coupled sine map. Here as well, the Lyapunov exponents and the unsynchronised, WS and SS dynamics were analysed.

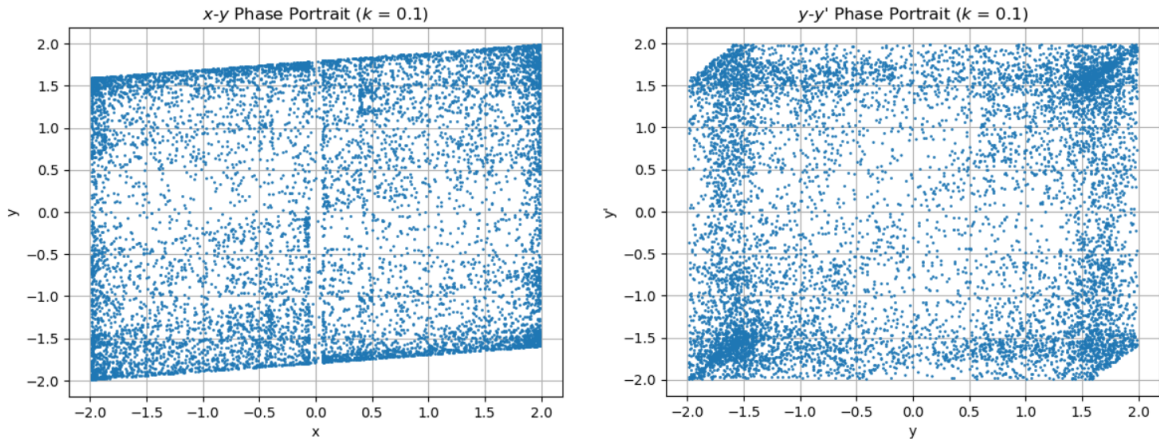


FIG. 15. Visualising the dynamics of a coupled sine system through phase portraits: The above plots showcase the  $x$ - $y$  and  $y$ - $y'$  dynamics when the system is unsynchronised at  $k = 0.100$  and  $r = 0.9$ .

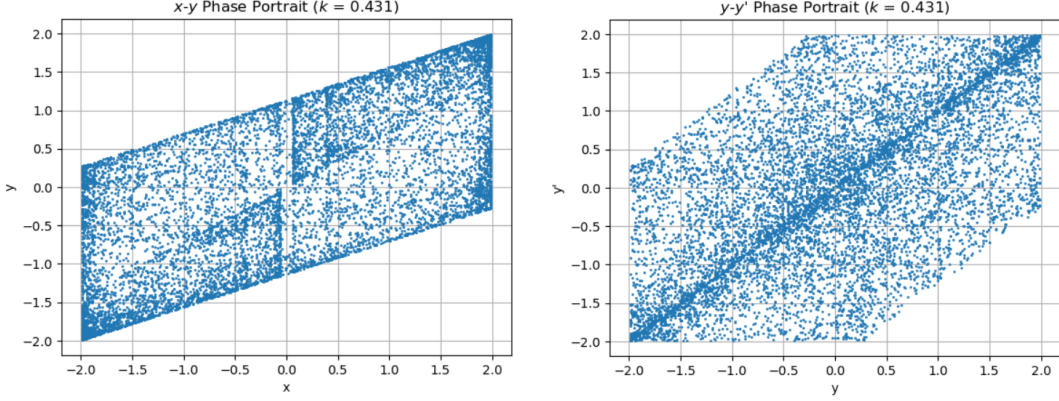


FIG. 16. Visualising the dynamics of a coupled sine system through phase portraits: The above plots showcase the  $x$ - $y$  and  $y$ - $y'$  dynamics when the system is weakly synchronised at  $k = 0.431$  and  $r = 0.9$ .

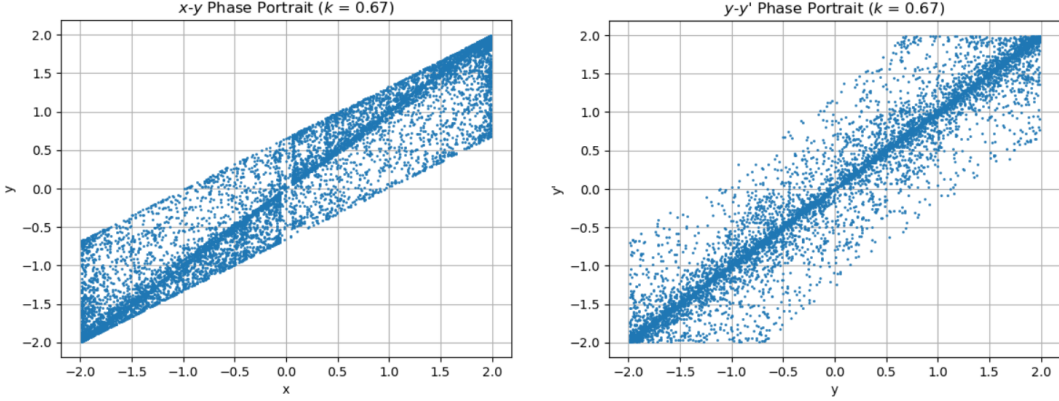


FIG. 17. Visualising the dynamics of a coupled sine system through phase portraits: The above plots showcase the  $x$ - $y$  and  $y$ - $y'$  dynamics when the system is strongly synchronised at  $k = 0.670$  and  $r = 0.9$ .

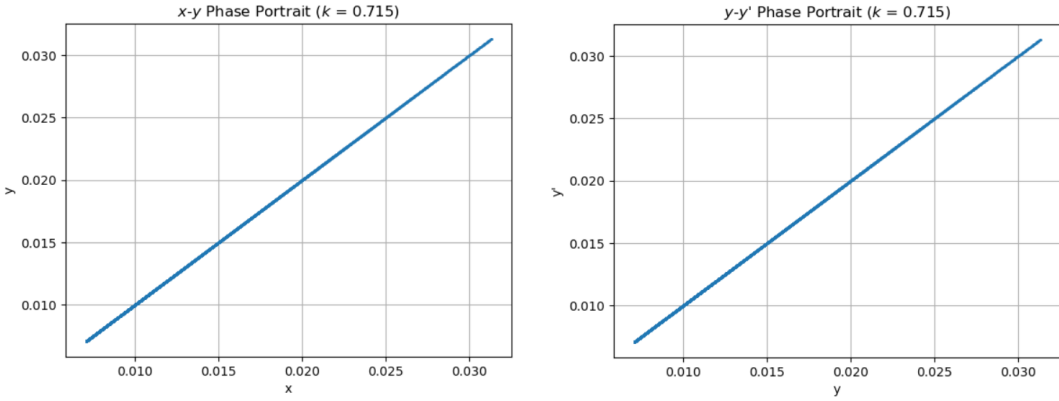


FIG. 18. Visualising the dynamics of a coupled sine system through phase portraits: The above plots showcase the  $x$ - $y$  and  $y$ - $y'$  dynamics when the system is strongly synchronised at  $k = 0.715$  and  $r = 0.9$ .

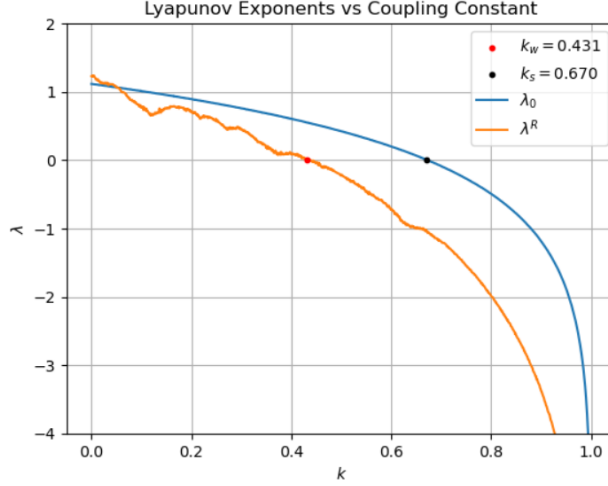


FIG. 19. Plotting the conditional (orange-coded) and transverse (blue-coded) Lyapunov exponents against each of the 1000  $k$  values considered with randomised initial conditions for the system. Here, the thresholds for the system are estimated to be  $k_w = 0.431$  and  $k_s = 0.670$  as they were found by eyeballing. Comparing the phase portraits at various  $k$  values with the thresholds found in this plot, one can see that there is a discrepancy in the SS threshold.

### III. THINGS TO DELVE FURTHER INTO

1. When observing the dynamics for the couple tent, cubic (see *Appendix*) and sine maps, apart from the characteristic phase plots for WS and SS, they have similar dynamics even for the unsynchronised case (a cube-like structure), despite different thresholds. Is it something trivial and expected, or is there some reason behind it?
2. Why do we see a discrepancy in the SS threshold for a coupled sine map?

- [1] K. Pyragas, “Weak and Strong Synchronization of Chaos,” Physical Review E, Vol. 54, No. 5, Nov. 1996.  
DOI: [10.1103/physreve.54.r4508](https://doi.org/10.1103/physreve.54.r4508).
- [2] S. H. Strogatz, *Nonlinear Dynamics and Chaos*, 2000, pp. 418–419. [Online] Available: [https://www.biodyn.ro/course/literatura/Nonlinear\\_Dynamics\\_and\\_Chaos\\_2018\\_Steven\\_H.\\_Strogatz.pdf](https://www.biodyn.ro/course/literatura/Nonlinear_Dynamics_and_Chaos_2018_Steven_H._Strogatz.pdf)

## APPENDIX

### A. Coupled Cubic Map: Lyapunov Exponents and Dynamics for Unsynchronised and SS Cases

A cubic map is defined by  $x_{n+1} = rx(1 - x^2)$  and plugging this into equation (1), we get the coupled cubic system.

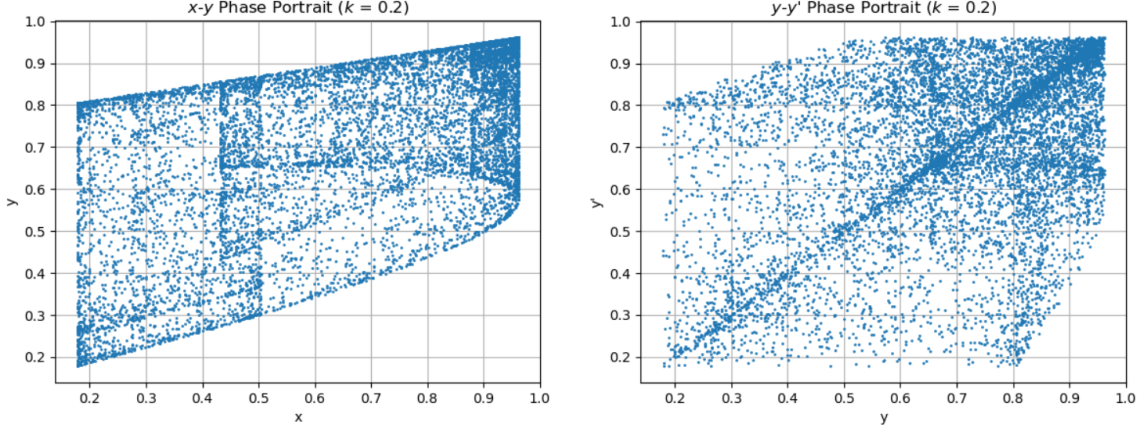


FIG. 20. Visualising the dynamics of a coupled cubic system through phase plots: The above plots showcase the  $x$ - $y$  and  $y$ - $y'$  dynamics when the system is unsynchronised at  $k = 0.2$  and  $r = 2.5$  (due to chaotic behaviour).

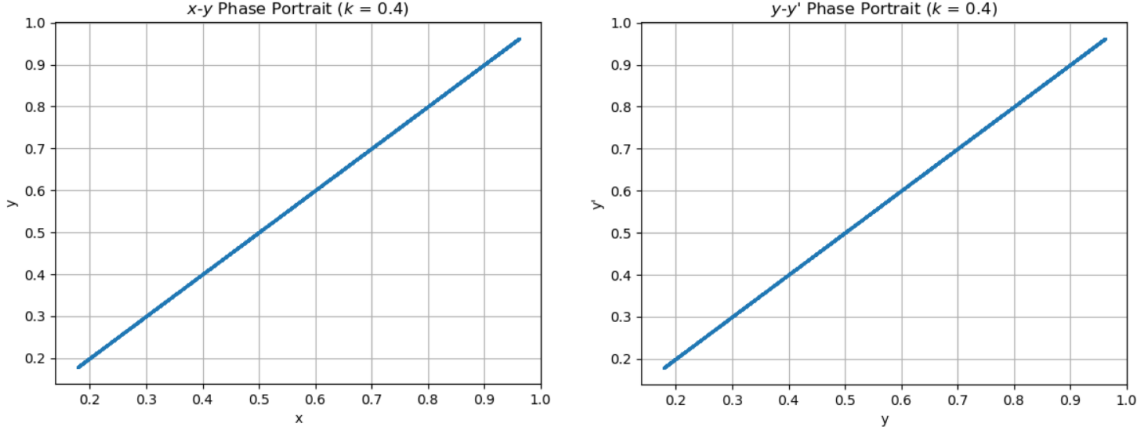


FIG. 21. Visualising the dynamics of a coupled cubic system through phase plots: The above plots showcase the  $x$ - $y$  and  $y$ - $y'$  dynamics when the system is strongly synchronised at  $k = 0.2$  and  $r = 2.5$  (due to chaotic behaviour).

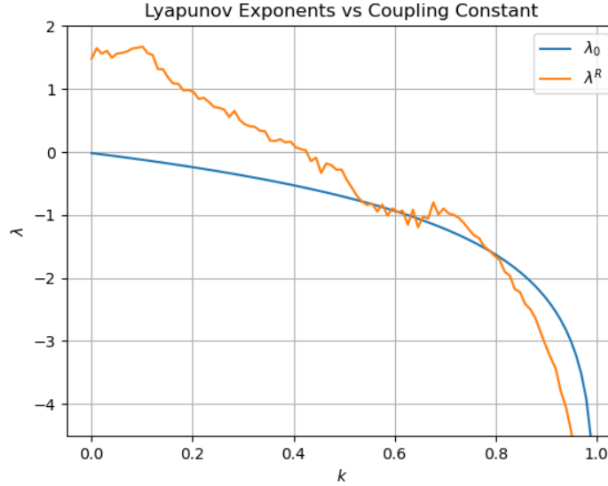


FIG. 22. Plotting the conditional and transverse Lyapunov exponents against the coupling strength  $k$  for the coupled cubic system. The curve is unusual as compared to the Lyapunov exponent curves for other systems explored in this report as the threshold for SS is less than the threshold for WS, and the transverse Lyapunov exponents are mostly negative, indicating a stable system. Therefore, whether this is the accurate curve or not is being determined.